Ocean Engineering 238 (2021) 109684

Contents lists available at ScienceDirect

Ocean Engineering

journal homepage: www.elsevier.com/locate/oceaneng

Barrier function-based adaptive neural network sliding mode control of autonomous surface vehicles

Yan Yan [a,*], Xiangtao Zhao [a], Shuanghe Yu [a,*], Chaoli Wang [b]

[a] College of Marine Electrical Engineering, Dalian Maritime University, Dalian 116026, China
[b] Department of Control Science and Engineering, University of Shanghai for Science and Technology, Shanghai 200093, China

ARTICLE INFO

Keywords:
Adaptive sliding mode control (SMC)
Barrier function (BF)
Neural networks (NNs)
Autonomous surface vehicles (ASVs)

ABSTRACT

In this paper, we consider trajectory tracking control for autonomous surface vehicles (ASVs) with unknown boundary model uncertainties and external disturbances. The neural networks (NNs) and the sliding mode control (SMC) with a switched adaptive law are combined for the first time. The NNs are used to approximate model uncertainties and external disturbances of ASVs. The parameters of the robust SMC term first increase until the sliding variable reaches a quasi sliding mode which bound is associated with the parameter of the barrier function (BF). Then the BF is selected as the parameter of the robust term for the SMC strategy to estimate the NN approximation error and to constrain the sliding variable inside the predefined quasi sliding mode. One salient feature of our approach is that the robust control parameter is no more than approximation error of NNs in sliding and steady phases of SMC. Simulation studies are performed to illustrate the advantage of the proposed control method.

1. Introduction

The autonomous surface vehicles (ASVs) have attracted much attention for various missions such as ocean surveillance, rescue and military tasks. Vehicle navigation can be classified into three basic problems: tracking a reference trajectory, following a path and point stabilization (Fierro and Lewis, 1998). For the path following control of surface vehicles, the vehicle is required to converge to and follow a path that is specified without a temporal law (Aguiar and Hespanha, 2007; Zheng and Sun, 2016; Xiang et al., 2017; Ghommam et al., 2018). The line-of-sight guidance law is commonly used for path following of ASVs (Fossen et al., 2003). Another tremendous practical application of the ASVs is to automatically track a time varying trajectory. In the application, the goal is to make the state of the ASV follow a reference or desired trajectory. However, the efficient tracking control design for ASVs is still a challenge problem for engineers and researchers due to the complex dynamics for the ocean vehicles, such as parameter variation and environmental disturbances (Wang and Han, 2018; Wu et al., 2018; Qiao and Zhang, 2019; Yu et al., 2019; Hu et al., 2020). Hence, the main purpose of the present paper is to propose a method to design controllers which achieves a trajectory tracking objective for ASVs affected by model uncertainties and external disturbances which are bounded with unknown boundary.

The sliding mode control (SMC) is a very effective robust control method due to its attractive properties including simple in control design and robust in parameter variations and disturbances (Edwards and Spurgeon, 1998; Yu et al., 2020). There are some significant results for the control of physical systems by using the SMC method (Ding et al., 2020; Du et al., 2019; Hou et al., 2020). In the past few years, the SMC approach has been used to the trajectory tracking control of ocean vehicles, for example, see Yan and Yu (2018) and Hao et al. (2020). However, the upper bounds of the matched model uncertainties and external disturbances should be assumed to be known previously before using the equivalent SMC (Utkin, 2013). Hence, most SMC methods for ocean vehicles are designed with the assumption that the upper bounds of the model uncertainties and external disturbances should be known. Nevertheless, in practical applications the upper bounds are not constants and often unknown. By using a dynamical adaptation of the control gain, the adaptive SMC methods are used to establish the sliding mode in finite time without a requirement to know the upper bound of the disturbances (Plestan et al., 2010). The barrier function (BF) can reach infinity while its arguments approaching the boundaries of constraints. By incorporating a BF in adaptive backstepping design, the constraints for the systems are not violated (Ngo et al., 2005; Tee et al., 2009; He et al., 2016). By adding a BF to the adaptive SMC law, the sliding variable can be maintained in a predefined neighborhood of zero without knowing the upper bound of disturbances (Obeid et al., 2018). In addition, the BF-based adaptive method is applied to the

* Corresponding authors.
E-mail addresses: y.yan@dlmu.edu.cn (Y. Yan), 1477856814@qq.com (X. Zhao), shuanghe@dlmu.edu.cn (S. Yu), clwang@usst.edu.cn (C. Wang).

https://doi.org/10.1016/j.oceaneng.2021.109684
Received 24 April 2021; Received in revised form 28 July 2021; Accepted 11 August 2021
Available online 27 August 2021

super-twisting systems (Obeid et al., 2020) and higher order SMC systems (Obeid et al., 2021; Laghrouche et al., 2021).

As another kind of adaptation strategy, neural networks (NNs) are used to approximate model uncertainties and external disturbances in trajectory tracking control of systems (Lewis et al., 1996; Wang and Huang, 2005; Sun et al., 2011; Mu et al., 2016; Wang et al., 2016; Liu et al., 2020; Zhou et al., 2020). The neural network (NN) is a useful tool in the adaptive control due to its learning ability to approximate arbitrary nonlinear functions. The SMC of the NN via event-triggered algorithm, time delay and quantization is given in Sun et al. (2020) and Wang et al. (2020). Adaptive neural control with the compensations of modeling uncertainties and external disturbances is developed in He et al. (2016) and Rout et al. (2020) to guarantee tracking performances for ocean vessels. The NN is adopted to approximate the complex hydrodynamics and differential of desired tracking velocities of underwater vehicles in Zhang et al. (2020). In Cui et al. (2017), adaptive-critic-based NN controllers are proposed for ASVs.

In this paper, we consider the design of a BF-based adaptive SMC law for trajectory tracking control of ASVs which are subject to model uncertainties and external disturbances with unknown boundary. The BF-based adaptive NN SMC strategy is composed of an equivalent SMC law, a NN and a switched adaptive law for the parameter of robust SMC term. The radial basis function (RBF) NN is used to approximate the model uncertainties and external disturbances. The robust control parameter increases first until the sliding variable reaches a quasi sliding mode region. Then a BF is selected as the parameter of the robust control term to estimate the NN approximation error and to prevent the sliding variable from steering out of the quasi sliding mode region. Compared with other NN SMC approaches, the adaptive law is switched according to the amplitude of the sliding variable. Then the parameter of the robust SMC term is no more than the approximation error of the NN in the sliding and steady phases of the SMC. The sliding variable and the tracking errors can converge to a bounded region related to the parameter of the BF. At last, comparative simulations with the BF-based SMC scheme are given using an ASV to show the superiority of the BF-based adaptive NN SMC strategy.

This paper is organized as follows. The dynamics of the ASV, the definition of the BF and the RBF NN are described in Section 2. The controller design and stability analysis are given in Section 3. Simulation results are provided in Section 4. Finally, conclusions are drawn in Section 5.

2. System dynamics and preliminaries

2.1. Kinematic and dynamic model of the ASV

The dynamics of the ASV are described by (Fossen, 2002)

$$\begin{aligned} \dot{\eta} &= R(\psi)\nu \\ M\dot{\nu} &= -C(\nu)\nu - D(\nu)\nu + \tau + d(t) \end{aligned} \tag{1}$$

where $\eta = [x, y, \psi]^T \in R^3$ is the position and posture vector, $\nu = [u, \upsilon, r]^T$ is the velocity vector, $\tau = [\tau_1, \tau_2, \tau_3]^T$ is the control vector consisting of surge force τ_1 and sway force τ_2 and yaw moment τ_3, $d(t) = [d_1(t), d_2(t), d_3(t)]^T$ is the disturbance vector consisting of equivalent disturbance forces $d_1(t)$ in surge, $d_2(t)$ in sway and the moment d_3 in yaw in the body-fixed frame. The rotation matrix R, the inertial matrix M, the Coriolis and centripetal matrix C, damping matrix D are given by

$$R(\psi) = \begin{bmatrix} \cos\psi & -\sin\psi & 0 \\ \sin\psi & \cos\psi & 0 \\ 0 & 0 & 1 \end{bmatrix}, \quad M = \begin{bmatrix} m - X_{\dot{u}} & 0 & 0 \\ 0 & m - Y_{\dot{\upsilon}} & mx_g - Y_{\dot{r}} \\ 0 & mx_g - N_{\dot{\upsilon}} & I_z - N_{\dot{r}} \end{bmatrix}$$

$$C(\nu) = \begin{bmatrix} 0 & 0 & c_{13}(\nu) \\ 0 & 0 & c_{23}(\nu) \\ -c_{13}(\nu) & -c_{23}(\nu) & 0 \end{bmatrix}, \quad D(\nu) = \begin{bmatrix} d_{11}(\nu) & 0 & 0 \\ 0 & d_{22}(\nu) & d_{23}(\nu) \\ 0 & d_{32}(\nu) & d_{33}(\nu) \end{bmatrix}$$

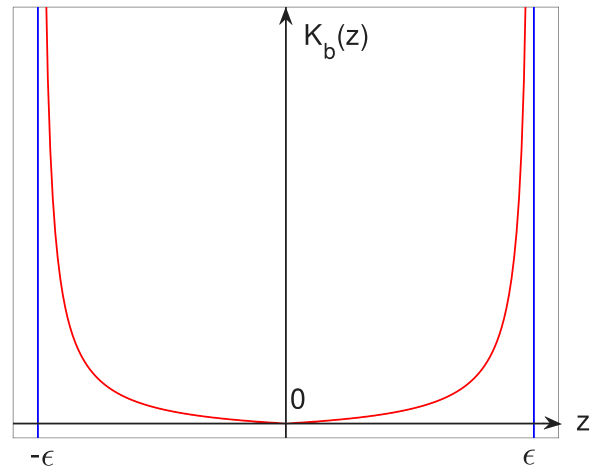

Fig. 1. Plot of function $K(z)$.

where m is the mass of vehicle, x_g is the distance between the center-of-gravity and the origin of body fixed frame, $Y_{\dot{r}} = N_{\dot{\upsilon}}$, I_z is the moment of inertia about the yaw rotation, $c_{13}(\nu) = -(m - Y_{\dot{\upsilon}})\upsilon - (mx_g - Y_{\dot{r}})$, $c_{23}(\nu) = (m - X_{\dot{u}})$, $d_{11}(\nu) = -X_u - X_{|u|u}|u|$, $d_{22}(\nu) = -Y_\upsilon - Y_{|\upsilon|\upsilon}|\upsilon| - Y_{|r|\upsilon}|r|$, $d_{23}(\nu) = -Y_r - Y_{|\upsilon|r}|\upsilon| - Y_{|r|r}|r|$, $d_{32}(\nu) = -N_\upsilon - N_{|\upsilon|\upsilon}|\upsilon| - N_{|r|\upsilon}|r|$, $d_{33}(\nu) = -N_r - N_{|\upsilon|r}|\upsilon| - N_{|r|r}|r|$ and the coefficients $\{X(\cdot), Y(\cdot), N(\cdot)\}$ are hydrodynamic parameters (Skjetne et al., 2004). Note that the rotation matrix has the properties $R(\psi)^T R(\psi) = I$ and $\|R(\psi)\| = I$, where $\|\cdot\|$ represents the 2-norm of a matrix or a vector.

The matrices C and D in (1) are considered as the unknown parts of the ASV dynamics. Let C_0 and D_0 be the nominal values of C and D. We have $C = \Delta C + C_0$ and $D = \Delta D + D_0$, where ΔC and ΔD are the uncertain parts of C and D, respectively. Then, the dynamic equations of the ASV in (1) can be written in the following form:

$$\begin{aligned} \dot{\eta} &= R(\psi)\nu \\ M\dot{\nu} &= -C_0(\nu)\nu - D_0(\nu)\nu + \tau - \Delta C(\nu)\nu - \Delta D(\nu)\nu + d(t) \end{aligned} \tag{2}$$

In this paper, the control objective is to develop a control input vector τ such that actual position vector of the ASV in (1) with unknown bounded model uncertainties and disturbances can track the desired trajectory vector $\eta_d(t)$ exactly. The following assumptions are made for system (2).

Assumption 1 (*Lewis et al., 1996*)**.** The upper bound of the parameter uncertainties and external disturbances is unknown. That is, there exists a constant L such that $\|-\Delta C(\nu)\nu - \Delta D(\nu)\nu + d(t)\| \le L$ but L is not known.

Assumption 2. The reference signal $\eta_d(t)$, $\dot{\eta}_d(t)$ and $\ddot{\eta}_d(t)$ are smooth and bounded.

2.2. Barrier function (BF)

In this paper, we consider the positive semi-definite BF with (Obeid et al., 2018)

$$K_b(z) = \frac{|z|}{\epsilon - |z|} \tag{3}$$

where $\epsilon > 0$ is the parameter of the BF. From (3), we can obtain $K_b(0) = 0$ and the property $K_b(z) \to \infty$ as z approaches $\pm\epsilon$. The plot of function $K_b(z)$ is shown in Fig. 1, where $z = -\epsilon$ and $z = \epsilon$ are vertical asymptotes.

2.3. RBF NN

RBF NNs are NNs that use RBF as the activation functions. Let U_x be a compact set of R^a. Let $f(x)$ be a smooth function from R^a to

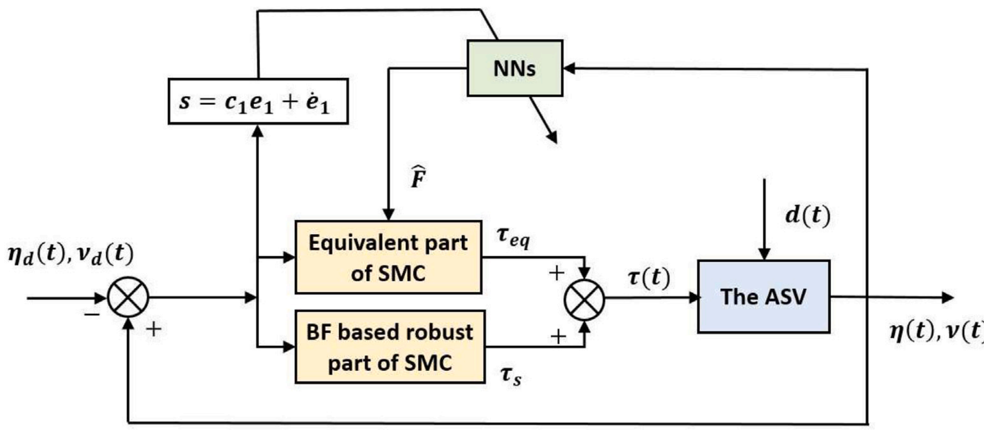

Fig. 2. Structure of the BF-based adaptive NN SMC system.

R^b. Define $W^* \in R^{l\times b}$ by the ideal weight matrix of the NN with the number of neurons in a hidden layer l. Then as long as x is restricted in U_x, the nonlinear function $f(x)$ with $x \in R^a$ can be approximated by the RBF NN as (Lewis et al., 1996)

$$f(x) = W^{*T}\phi(x) + \delta \tag{4}$$

where $x \in R^a$ is the input vector, $\phi(x) = [\phi_1(x), \phi_2(x), \ldots, \phi_l(x)]^T$ and $\delta = [\delta_1, \delta_2, \ldots, \delta_b]^T$ is the network reconstruction error vector. In addition, one can find a NN such that $\|\delta\| \le \delta_N$ holds for any choice of a positive constant δ_N in U_x. Let $\phi_j(x)$ be the Gaussian function. Then we have

$$\phi_j(x) = \exp\left(-\frac{\|x-\mu_j\|^2}{2\sigma^2}\right), \quad j = 1, 2, \ldots, l \tag{5}$$

where $\mu_j = [\mu_{j1}, \mu_{j2}, \ldots, \mu_{ja}]^T$ is the center of the Gaussian function and $\sigma > 0$ is the width of the Gaussian function.

Noting that W^* is unknown, we need to estimate W^* online. Let $\hat{W}$ be the estimation of W^*. We will design an adaptive law to update $\hat{W}$ in the next section.

Assumption 3. The ideal weights are bounded by known positive values so that $\|W^*\|_F \le W_M$.

3. BF-based adaptive NN SMC design with modeling uncertainties and disturbances

This section will give the design of a BF-based adaptive NN SMC law. The block diagram of the control system is shown in Fig. 2, where $\eta = [x, y, \psi]^T$ is the position and posture vector, $\nu = [u, v, r]^T$ is the velocity vector and τ is control input. Let $\eta_d(t)$ and $\nu_d(t)$ denote the desired position and velocity vectors, respectively. The NN is used to approximate the modeling uncertainties and the external disturbances. The NN output is denoted as $\hat{F}$. Let s be the designed sliding variable. Note that the SMC law τ in Fig. 1 is composed of the equivalent control term τ_{eq} and the robust control term τ_s which will be introduced later.

We define the tracking errors by

$$e_1 = \eta - \eta_d(t), \quad e_2 = \dot{\eta} - \dot{\eta}_d(t) \tag{6}$$

Noting $\dot{R} = RS$ with $S = [0\ \ -r\ 0; r\ 0\ 0; 0\ 0\ 0]$ and recalling (2), we obtain the dynamics of tracking errors as follows

$$\begin{aligned} \dot{e}_1 &= e_2 \\ \dot{e}_2 &= RS(\nu)\nu + F + RM^{-1}\left(-C_0(\nu)\nu - D_0(\nu)\nu + \tau\right) - \ddot{\eta}_d(t) \end{aligned} \tag{7}$$

where $F = RM^{-1}\left(-\Delta C(\nu)\nu - \Delta D(\nu)\nu + d(t)\right)$.

Choose the following sliding variable

$$s = c_1 e_1 + e_2 \tag{8}$$

where the constant $c_1 > 0$ is the parameter of sliding variable and e_1 and e_2 are given in (6). By using the equivalent SMC method (Utkin, 2013), the control law can be chosen as the following form

$$\tau = \tau_{eq} + \tau_s \tag{9}$$

with

$$\tau_{eq} = \left(C_0(\nu) + D_0(\nu)\right)\nu - MR^{-1}\left(\hat{F} + c_1 e_2 + RS(\nu)\nu - \ddot{\eta}_d\right) \tag{10}$$

$$\tau_s = -MR^{-1}K(t, s(t))\mathrm{sgn}(s) \tag{11}$$

where τ_{eq} is the equivalent control term, $\hat{F}$ is an estimate of F provided by the NN, τ_s is the robust control term and $K(t, s(t)) = \mathrm{diag}\{K_1(t, s_1(t)), K_2(t, s_2(t)), K_3(t, s_3(t))\}$ is the adaptive parameter matrix. The sign function $\mathrm{sgn}(\cdot)$ is defined as $\mathrm{sgn}(z) = 1$ if $z > 0$, $\mathrm{sgn}(z) = 1$ if $z < 0$, $\mathrm{sgn}(z) \in [-1, 1]$ if $z = 0$ for a scalar $z \in R$ and operated element-wise for a vector $z \in R^n$ (Shtessel et al., 2014).

Suppose that there exists a constant ideal weight matrix W^* such that F can be written as

$$F = W^{*T}\phi(x) + \delta \tag{12}$$

where $x = \nu \in R^3$ is the NN input vector and $W^* \in R^{l*3}$ with the number of neurons in the hidden layer l. Here we use the RBF network to approximate F in (7). The output of the NN can be expressed by

$$\hat{F} = \hat{W}^T\phi(x) \tag{13}$$

where $\hat{W}$ is the estimation of the NN weight W^*, $\phi(x) = [\phi_1(x), \phi_2(x), \ldots, \phi_l(x)]^T$ and $\phi_j(x)$ is the Gaussian function as given in (5) for $j = 1, 2, \ldots, l$.

The time derivative of (8) along (7) becomes

$$\begin{aligned} \dot{s} &= c_1 e_2 + \dot{e}_2 \\ &= c_1 e_2 + RS(\nu)\nu + F + RM^{-1}\left(-C_0(\nu)\nu - D_0(\nu)\nu + \tau\right) - \ddot{\eta}_d \end{aligned} \tag{14}$$

Substituting (9) into (14) and from $\hat{F} = \hat{W}^T\phi(x)$ as given in (13), the dynamics of s can be rewritten as

$$\dot{s} = \tilde{W}^T\phi(x) + \delta - K(t, s(t))\mathrm{sgn}(s) \tag{15}$$

where $\tilde{W} = W^* - \hat{W}$ is the weight estimation error of the RBF network.

In this paper, the parameter of the robust term in the equivalent SMC method given in (11) is dynamically turned to make sure the sliding variable s_i reaches the region $|s_i| \le \epsilon$, where $\epsilon > 0$ is the parameter of BF as given in (3). Then the gain is switched to the BF in order to counteract the approximation errors of the RBF NN. Moreover, the BF can prevent the siding variable s_i from reaching the upper bound of the quasi sliding mode $|s_i| = \epsilon$ for $i = 1, 2, 3$. The next theorem gives the main content in this paper.

Theorem 1. *Consider the ASV (1) with bounded initial conditions, as well as unknown parameter uncertainties and external disturbances which satisfy Assumptions 1–3 and the control input (9). The NN weight update law and the adaptive control gain $K(t,s(t))$ of the robust control term τ_s as given in (11) are chosen as*

$$\dot{\hat{W}} = \Gamma\phi(x)s^T \tag{16}$$

$$K_i(t,s_i(t)) = \begin{cases} K_{ai}(t),\ \dot{K}_{ai}(t) = \bar{K}\,|s_i(t)|\,, & \text{if } 0<t\le \bar{t}_i \\ K_{bi}(s_i(t)), & \text{if } t>\bar{t}_i \end{cases} \tag{17}$$

where $\Gamma = diag[\Gamma_1,\Gamma_2,\dots,\Gamma_l] > 0$ is any constant matrix, $\bar{K}>0$ is a positive constant, $K_{bi}(s_i) = \frac{|s_i|}{\epsilon-|s_i|}$ with the parameter of the BF $\epsilon>0$, $\bar{t}_i$ is the smallest root of $|s_i| < \frac{\epsilon}{2}$ and $i=1,2,3$. Given any positive number $V_m>0$, for all initial conditions satisfying $\sum_{i=1}^{3}\left(s_i^2+\frac{1}{\gamma}(K_{ai}-K_i^*)^2+\frac{1}{\Gamma_i}\tilde{W}_i^T\tilde{W}_i\right)\le 2V_m$ with a constant $K_i^*>K_{ai}$, then neural network weight estimation error $\tilde{W}$ and all system states are uniformly ultimate bounded. Moreover, the system state can reach the region $\|s\|<\sqrt{3}\epsilon$ and stay in it thereafter. The tracking errors of the ASV can converge to the region $\|e_1\|\le\sqrt{3}\epsilon/c_1$.

Proof. The proof is composed of two steps. The first step concerns that $|s_i|$ will reach $\frac{\epsilon}{2}$ in finite time $\bar{t}_i$, whereas the second one concerns that s_i can coverage to $|s_i|<\epsilon$ in finite time for $t\ge\bar{t}_i$ and $|s_i(t)|>s_a$, where $0<s_a<\epsilon$ and $i=1,2,3$.

Step 1: If $|s_i(0)|<\frac{\epsilon}{2}$, then we enter the Step 2 directly with $\bar{t}_i=0$. According to the Lemma 1 in Plestan et al. (2010), there exists a constant $K^*>0$ such that

$$K_{ai} < K^*, \quad \forall\, t>0 \tag{18}$$

When $0\le t\le\bar{t}_i$ for $i=1,2,3$, select the Lyapunov function

$$V_{ai} = \frac{1}{2}s_i^2 + \frac{1}{2\gamma}(K_{ai}-K_i^*)^2 + \frac{1}{2\Gamma_i}\tilde{W}_i^T\tilde{W}_i \tag{19}$$

where γ is a positive constant satisfying $0<\gamma<\bar{K}$, K^* is given in (18) and $\hat{W}_i\in R^{l*1}$ is the ith column of $\hat{W}$. Eq. (15) can be rewritten as

$$\dot{s}_i = \tilde{W}_i^T\phi(x)+\delta_i - K_i(t,s_i(t))\mathrm{sgn}(s_i),\ \ i=1,2,3 \tag{20}$$

Differentiating (19) along (17) and (20), we have

$$\begin{aligned}\dot{V}_{ai} &= s_i\dot{s}_i + \frac{1}{\gamma}(K_{ai}-K_i^*)\dot{K}_{ai} + \tilde{W}_i^T\cdot\frac{\dot{\tilde{W}}_i}{\Gamma_i} \\ &= -s_iK_i(t,s_i(t))\mathrm{sgn}(s_i) + \frac{1}{\gamma}(K_{ai}-K_i^*)\dot{K}_{ai} + \tilde{W}_i^T\left(\frac{\dot{\tilde{W}}_i}{\Gamma_i}+s_i\phi(x)\right)+s_i\delta_i\end{aligned} \tag{21}$$

Note that the third term in the last equation is zero if we select

$$\dot{\tilde{W}}_i = -\Gamma_i\phi(x)s_i,\ \text{ for } i=1,2,3 \tag{22}$$

Since $\tilde{W}_i = W_i^* - \hat{W}_i$ and W_i^* is a constant, then $\dot{\tilde{W}}_i = -\dot{\hat{W}}_i$ and the NN update law (16) are obtained.

According to (17) and (20)–(22), the time derivative of V_{ai} yields

$$\begin{aligned}\dot{V}_{ai} &= s_i\dot{s}_i + \frac{1}{\gamma}(K_{ai}-K_i^*)\dot{K}_{ai} - \tilde{W}_i^T\dot{\hat{W}}_i \\ &= s_i\delta - K^*|s_i| + K^*|s_i| - K_{ai}|s_i| + \frac{\bar{K}}{\gamma}(K_{ai}-K^*)|s_i| \\ &\le -(K^*-\delta_N)|s_i| - (\frac{\bar{K}}{\gamma}-1)(K^*-K_{ai})|s_i|\end{aligned} \tag{23}$$

Note that the terms $|\tilde{W}_i^T\phi(x)+\delta_i|\le\Psi$ in (20) with unknown upper bound $\Psi>0$. According to Lemma 1 in Plestan et al. (2010), K_{ai} is increasing and there exists a time t_1 such that $K_{ai}>\Psi\ge\delta_N$. From $K^*>K_{ai}$ and $0<\gamma<\bar{K}$, we obtain that always exists K^* such that $K^*-\delta_N>0$ and $(\frac{\bar{K}}{\gamma}-1)(K^*-K_{ai})>0$ for all $t>0$. It yields $\dot{V}_{ai}\le 0$. Then we obtain that s_i, $K_{ai}-K^*$ and $\tilde{W}_i$ are bounded. Note that $\dot{V}_{ai}\le 0$ is not necessary for s_i to reach zero in finite time. Hence, we use another Lyapunov function as

$$V_{a1i} = \frac{1}{2}s_i^2 + \frac{1}{2\gamma}(K_{ai}-K_i^*)^2 \tag{24}$$

Differentiating (24) with respect to time and using (20), we obtain

$$\begin{aligned}\dot{V}_{a1i} &= s_i\dot{s}_i + \frac{1}{\gamma}(K_{ai}-K^*)\dot{K}_{ai} \\ &\le \left(\tilde{W}_i^T\phi_i(x)+\delta_N-K_{ai}\right)|s_i| + K^*|s_i| - K^*|s_i| + \frac{1}{\gamma}(K_{ai}-K^*)\bar{K}|s_i| \\ &\le -\underbrace{(K^*-\delta_N-\|\tilde{W}_i^T\phi_i(x)\|)}_{\beta_a}|s_i| - \underbrace{(\frac{\bar{K}}{\gamma}-1)|s_i|}_{\beta_b}|K^*-K_{ai}|\end{aligned} \tag{25}$$

Observe that the Gaussian function $\phi_i(x)$ is bounded by $0<\phi_i(x)<1$. It follows that $\|\tilde{W}_i^T\phi_i(x)\|\le\|\tilde{W}_i^T\|$. There always exist K^* and γ such that $K^*>\delta_N+\|\tilde{W}_i^T\phi_i(x)\|$ and $\gamma<\bar{K}$. It follows that $\beta_a>0$ and $\beta_b>0$. Then we have

$$\begin{aligned}\dot{V}_{a1i} &\le -\beta_a|s_i| - \beta_b|K^*-K_{ai}| \\ &= -\beta_a\sqrt{2}\frac{|s_i|}{\sqrt{2}} - \beta_b\sqrt{2\gamma}\frac{|K^*-K_{ai}|}{\sqrt{2\gamma}} \\ &\le -\min\{\beta_a\sqrt{2},\beta_b\sqrt{2\gamma}\}\left(\frac{|s_i|}{\sqrt{2}},\frac{|K^*-K_{ai}|}{\sqrt{2\gamma}}\right) \le -\beta_1V_{a1i}^{1/2}\end{aligned} \tag{26}$$

where $\beta_1 = \min\{\beta_a\sqrt{2},\beta_b\sqrt{2\gamma}\}$. Thus, it can be concluded that $|s_i(t)|$ can converge to zero in finite time. Moreover, there exists $\bar{t}_i\ge 0$ such that $\bar{t}_i$ is the smallest root of $|s_i|=\frac{\epsilon}{2}$ for $i=1,2,3$.

Step 2: When $t>\bar{t}_i$ with $|s_i(\bar{t}_i)|=\frac{\epsilon}{2}$ for $i=1,2,3$, choose the Lyapunov function

$$V_{bi} = \frac{1}{2}s_i^2 + \frac{1}{2}K_{bi}^2(s_i) + \frac{1}{2\Gamma_i}(\tilde{W}_i^T\tilde{W}_i) \tag{27}$$

Substituting (17), (20) and (22) into the derivative of (27) yields

$$\begin{aligned}\dot{V}_{bi} &= s_i\left(\tilde{W}_i^T\phi(x)+\delta_i-K_{bi}(t,s_i(t))\mathrm{sgn}(s_i)\right) + K_{bi}\dot{K}_{bi} - \frac{1}{\Gamma_i}\tilde{W}_i^T\left(\Gamma_i\phi(x)s_i\right) \\ &= s_i(\delta_i - K_{bi}\mathrm{sgn}(s_i)) + K_{bi}(s_i)\frac{\epsilon}{(\epsilon-|s_i|)^2}\left(\mathrm{sgn}(s_i)\xi_i - K_{bi}(s_i)\right) \\ &\le -(K_{bi}(s_i)-\delta_N)|s_i| - \frac{\epsilon}{(\epsilon-|s_i|)^2}(K_{bi}(s_i)-|\xi_i|)|K_{bi}(s_i)|\end{aligned} \tag{28}$$

where $\xi_i = \tilde{W}_i^T\phi_i(x)+\delta$. Denote

$$s_{ai} = \epsilon\frac{|\xi_i|}{|\xi_i|+1} \tag{29}$$

Note that $s_{ai}<\epsilon$ for any $|\xi_i|\ge 0$. From (3) and Fig. 1, we get $K_{bi}(s_i)>K_{bi}(s_a)=|\xi_i|\ge\delta_N$ when $|s_i(t)|>s_{ai}$. According to the last inequality of (28), it follows that $\dot{V}_{bi}\le 0$ and s_i, K_{bi} and $\tilde{W}_i$ are bounded in the condition $|s_i(t)|>s_{ai}$.

According to Lemma 6 in Obeid et al. (2018), the next Lyapunov function is used to prove that s_i can converge to $|s_i|\le s_a$ in a finite time T_i for $i=1,2,3$.

$$V_{b1i} = \frac{1}{2}s_i^2 + \frac{1}{2}K_{bi}(s_i(t))^2 \tag{30}$$

Differentiating (30) with respect to time leads to

$$\begin{aligned}\dot{V}_{b1i} &= s_i\dot{s}_i + K_{bi}\dot{K}_{bi} \\ &= s_i\left(\tilde{W}_i^T\phi_i(x)+\delta_i\right) - K_{bi}|s_i| \\ &+ \frac{\epsilon K_{bi}}{(\epsilon-|s_i|)^2}\left(\mathrm{sgn}(s_i)(\tilde{W}_i^T\phi_i(x)+\delta) - K_{bi}\right) \\ &\le -\underbrace{\left(K_{bi}(s_i)-|\xi_i|\right)}_{\beta_c}|s_i| - \underbrace{(K_{bi}(s_i)-|\xi_i|)\frac{\epsilon}{(\epsilon-|s_i|)^2}}_{\beta_d}|K_{bi}(s_i)|\end{aligned} \tag{31}$$

Table 1
Dynamic parameters of the Cybership II.

Parameter	Value	Parameter	Value	Parameter	Value
m	23.8	x_g	0.046	I_z	1.76
$X_{\dot{u}}$	−2.0	$Y_{\dot{v}}$	−10.0	$Y_{\dot{r}}$	−0.0
$N_{\dot{v}}$	−0.0	$N_{\dot{r}}$	−1.0	X_u	−0.7225
$X_{\|u\|u}$	−1.3274	X_{uuu}	−5.8664	Y_v	−0.8896
$Y_{\|v\|v}$	−36.4728	N_v	0.0313	$N_{\|v\|v}$	3.9564
$Y_{\|r\|v}$	−0.805	Y_r	−7.25	$Y_{\|v\|r}$	−0.845
$Y_{\|r\|r}$	−3.45	$N_{\|r\|v}$	0.13	N_r	−1.9
$N_{\|v\|r}$	0.08	$N_{\|r\|r}$	−0.750		

Noting $K_{bi}(s_i) > K_{bi}(s_a)$ when $|s_i| > s_a$ and from $K_{bi}(s_a) = |\xi_i| \geq \delta_N$, we obtain $\beta_c > 0$ and $\beta_d > 0$ when $|s_i| > s_a$. It follows that

$$\dot{V}_{b1i} \leq -\min\{\beta_c\sqrt{2}, \beta_d\sqrt{2}\}\left(\frac{|s_i|}{\sqrt{2}}, \frac{|K_{bi}(s_i)|}{\sqrt{2}}\right) \leq -\beta_2 V_{b1i}^{1/2} \tag{32}$$

where $\beta_2 = \min\{\beta_c\sqrt{2}, \beta_d\sqrt{2}\}$.

Hence, after $t = \bar{t}_i$, s_i can converge to the region $|s_i| \leq s_a$ in finite time

$$T_i = \frac{2}{\beta_2}\left(V_{b1i}^{\frac{1}{2}}(s_i(\bar{t}_i), K_{bi}(s_i(\bar{t}_i))) - V_{b1i}^{\frac{1}{2}}(s_a, K_{bi}(s_a))\right) \tag{33}$$

where $i = 1, 2, 3$. According to (26) and (33), s converges to the region $\|s\| \leq \sqrt{3}s_a$ in finite time $t = \max\{\bar{t}_1 + T_1, \bar{t}_2 + T_2, \bar{t}_3 + T_3\}$. Noting $\|e_1\| \leq \|s\|/c_1$, it follows that the bound of tracking error e_1 is $\|e_1\| \leq \frac{\sqrt{3}s_a}{c_1}$. The Theorem 1 is proven. □

Remark 1. From Theorem 1, the BF parameter ϵ affects the upper bound of the quasi-sliding mode and tracking accuracy. That is, $\|s\| = O(\epsilon)$ and $\|e\| = O(\epsilon)$.

Remark 2. For the BF-based adaptive SMC method (Obeid et al., 2018), after $t_i = \bar{t}_i$, the adaptive gain K_i decreases until the value allows to compensate model uncertainties and disturbances F_i with $F = RM^{-1}\left(-\Delta C(\nu)\nu - \Delta D(\nu)\nu + d(t)\right)$ as given in (7). By using the BF-based adaptive NN SMC strategy given in Theorem 1, after $t_i = \bar{t}_i$, the adaptive gain K_i decreases till the value can compensate the term $\tilde{W}_i^T\phi(x) + \delta_i$ as shown in (20) for $i = 1, 2, 3$.

Remark 3. When $t \geq \bar{t}_i$, from $\frac{|s_i|}{\epsilon - |s_i|}\text{sgn}(s_i) = \frac{s_i}{\epsilon - |s_i|}$, we obtain that the control input of the ASV is continuous (Obeid et al., 2018) and the dynamics of s_i becomes $\dot{s}_i = \tilde{W}_i^T\phi(x) + \delta_i - \frac{1}{\epsilon - |s_i|}s_i$ for $i = 1, 2, 3$.

4. Simulations

In this section, we use a well-known ASV named CyberShip II to show the effectiveness of the proposed controller. The model parameters of CyberShip II can be found in Table 1 (Skjetne et al., 2004). The reference trajectory is given as $\eta_d(t) = [6\sin(0.02t), 0.25(1 - \cos(0.02t)), 0.02t]^T$. The initial condition of the ASV is $\eta(0) = [0.3, 0.5, \pi/4]^T$ and $\nu(0) = [0, 0, 0]^T$. Let the model uncertainties and time-varying disturbances introduced into the model be $-\Delta C(\nu)\nu - \Delta D(\nu)\nu = [0.7u^2 vr, 0.9u^3 v, 0.8u^2 v + 0.142v^2]^T$ and $d = [3\cos(t)\cos(0.5t) + 2\sin(0.3t)\cos(0.8t) - 1, 4\cos(t) - 0.6 + 3\sin(0.03t - \pi/8)\cos(0.5t), 5\sin(t)\cos(0.2t) + 4\cos(0.1t)]^T$ (Wang and Pan, 2019).

We apply the SMC (9) with the BF-based adaptive law (17) to achieve the control objective. The BF parameter is chosen as $\epsilon = 0.1$. The sliding variable parameter is selected as $c_1 = 15$. We set $\bar{K} = 0.05$ and $K_{ai}(0) = 0.1$ to prevent the value of K_{ai} from increasing too fast during $0 < t \leq \bar{t}_i$ $(i = 1, 2, 3)$. For the adaptive law, the number of neurons in the hidden layer is chosen as $l = 15$. The RBF widths are 5 and the centers are evenly spaced on $[-0.7, 0.7]$. By using the same system parameters, the control tasks, model uncertainties and disturbances, the initial conditions, the BF and the controller parameters, we compare the performance between the BF-based adaptive NN SMC (BF NN SMC) proposed in this paper and a BF-based adaptive SMC (BF SMC) designed in Obeid et al. (2018).

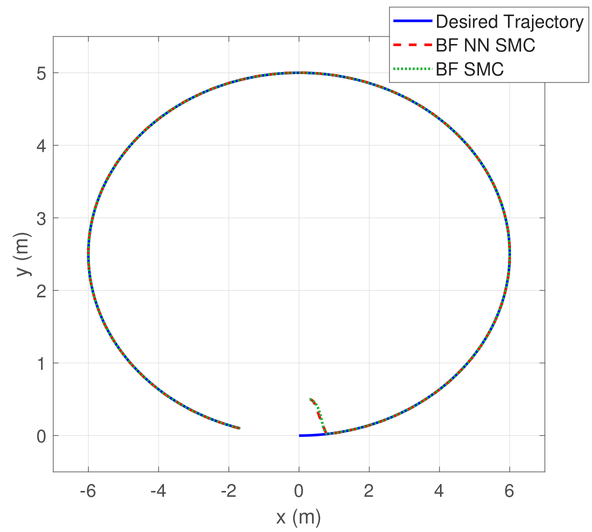

Fig. 3. Desired trajectory and actual trajectories in the xy plane.

The simulation results under the BF NN SMC and BF SMC are presented in Figs. 3–10. Fig. 3 shows the desired and actual trajectories of the ASVs in the horizontal plane. Denote $F = RM^{-1}\left(-\Delta C(\nu)\nu - \Delta D(\nu)\nu + d\right)$ with $F = [F_1, F_2, F_3]^T$. F is plotted in Fig. 4 by using black lines whereas the outputs of the NNs are plotted by using red dash lines. It demonstrates that unknown model uncertainties and disturbances are efficiently compensated by the proposed RBF NN.

The performances of the adaptive parameters K_1, K_2 and K_3 with NN and without NN are illustrated in Fig. 5. It can be seen that the absolutely values of K_i decrease dramatically by using BF NN SMC for $i = 1, 2, 3$. This is due to that K_i is used to compensate the NN approximation error for BF NN SMC whereas K_i is used to compensate the unknown model uncertainties and disturbances for BF SMC as given in Remark 2. Furthermore, the adaptive control parameter K_i for BF NN SMC is an increasing function when $t_i \leq \bar{t}_i$ with $\bar{t}_1 = 6.077$, $\bar{t}_2 = 6.253$ and $\bar{t}_3 = 7.411$ as illustrated in Fig. 5.

Figs. 6–7 show that the sliding variable s_i can converge to the quasi-sliding mode bound $|s_i| < \epsilon$ when using BF NN SMC and BF SMC. It can be observed that after reaching $|s_i| < \epsilon$ the oscillation amplitude of s_i by using BF SMC is greater than that by using BF NN SMC. This verifies the description that for $|s_i| < \epsilon$ control input is continuous as shown in Remark 3. In addition, the term $\tilde{W}_i^T\phi(x) + \delta_i$ and the term F affect the oscillation amplitude of s_i for BF NN SMC and BF SMC, respectively. By comparing Figs. 8 and 9, it can be seen that the chattering amplitudes of the attitude tracking error e_1 for the NN BF SMC are smaller than that for the BF SMC.

The control inputs τ_i with NN and without NN are given in Fig. 10 for $i = 1, 2, 3$. The red and blue lines represent the behaviors of the BF NN SMC system and the BF SMC system, respectively. Fig. 10 shows that the control input τ_i becomes continuous when $t > \bar{t}_i$ for $i = 1, 2, 3$ as given in Remark 3.

5. Conclusion

In this paper, a BF-based adaptive NN SMC scheme has been proposed for the trajectory tracking control of the ASV which has model uncertainties and disturbances with unknown upper bound. A NN, a BF-based switched adaptive law and the equivalent SMC approach have been combined. The RBF NN has been introduced to approximate the unknown disturbances and model uncertainties. In the sliding and

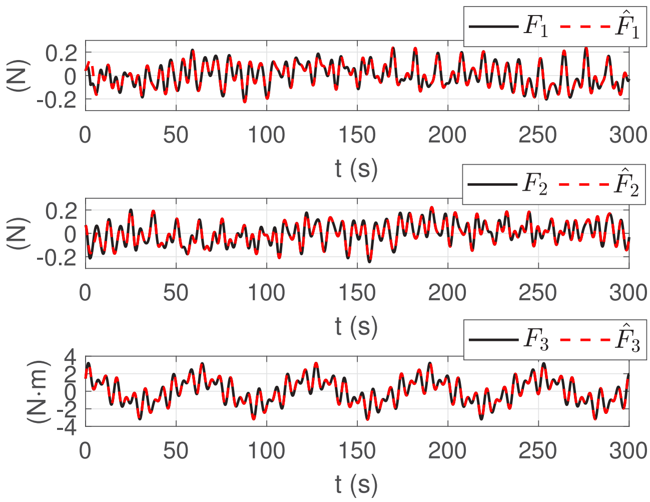

Fig. 4. Approximation of the unknown disturbances and model uncertainties by using NNs.

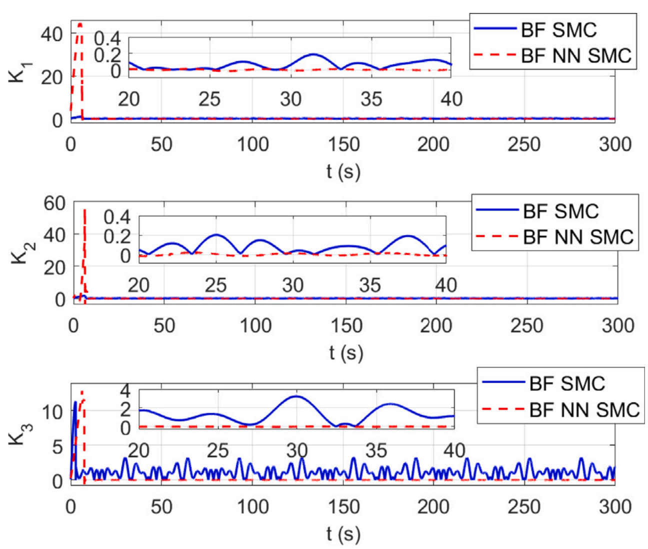

Fig. 5. Comparison of the adaptive SMC parameters K_1, K_2 and K_3 by using BF SMC and BF NN SMC.

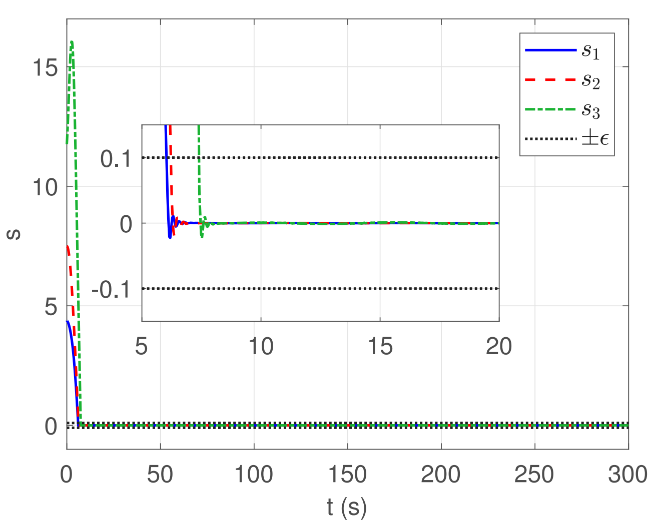

Fig. 6. Sliding variable s by using BF NN SMC.

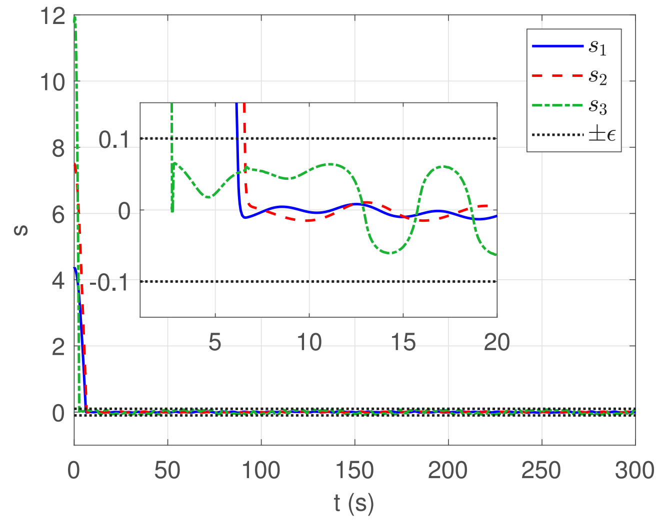

Fig. 7. Sliding variable s by using BF SMC.

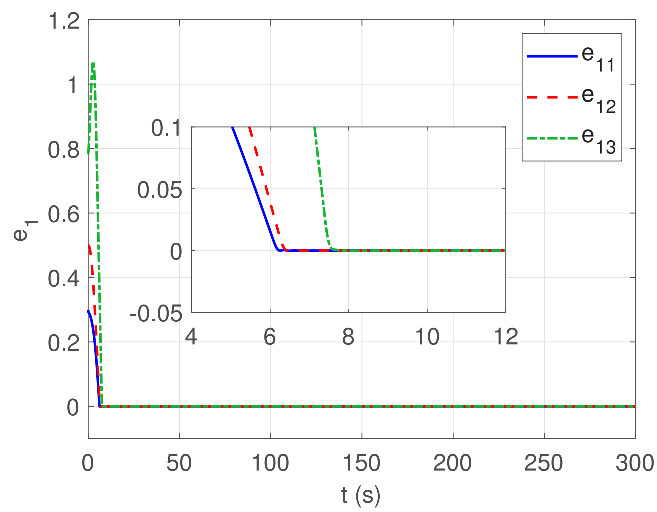

Fig. 8. The attitude tracking error e_1 by using BF NN SMC.

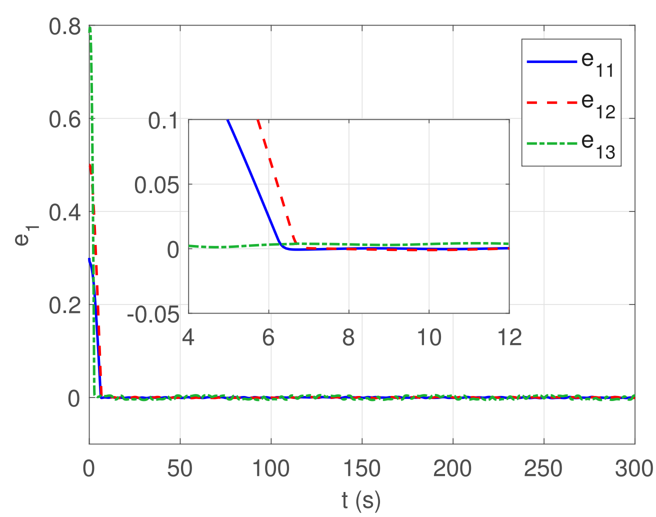

Fig. 9. The attitude tracking error e_1 by using BF SMC.

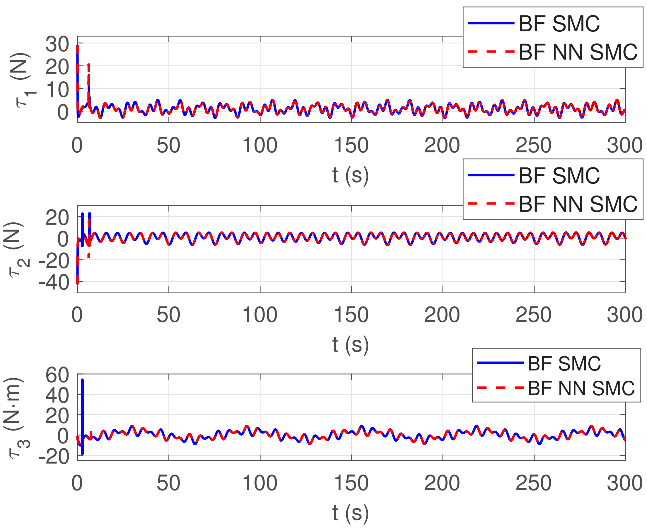

Fig. 10. Comparison of the control inputs by using BF SMC and BF NN SMC.

steady phases of SMC, the BF has been selected as the parameter of the robust SMC term to estimate the NN approximation error and to prevent the sliding variable from steering out of the quasi sliding mode. In addition, by using Cybership II, comparative studies between the proposed strategy and the BF-based adaptive SMC law have shown the effectiveness of the proposed scheme. Future research will extend the proposed method to address the ASV with input saturation and formation control of multiple ASVs, as well as on experimental validating the advanced algorithms.

CRediT authorship contribution statement

Yan Yan: Software, Writing - original draft, Methodology, Funding acquisition. **Xiangtao Zhao:** Software, Writing - original draft, Methodology. **Shuanghe Yu:** Writing - review & editing, Formal analysis, Supervision, Validation. **Chaoli Wang:** Writing - review & editing, Formal analysis, Validation.

Declaration of competing interest

The authors declare that they have no known competing financial interests or personal relationships that could have appeared to influence the work reported in this paper.

Acknowledgments

This work was supported in part by the Natural Science Foundation of China under Grant 62073054, in part by China Postdoctoral Science Foundation under Grant 2020M680930, in part by the Dalian Innovative Support Scheme for High-Level Talents, China under Grant 2019RQ092 and in part by the Natural Science Foundation of Shanghai, China 19ZR1436000.

References

Aguiar, A.P., Hespanha, J.P., 2007. Trajectory-tracking and path-following of under-actuated autonomous vehicles with parametric modeling uncertainty. IEEE Trans. Automat. Control 52 (8), 1362–1379.
Cui, R., Yang, C., Li, Y., Sharma, S., 2017. Adaptive neural network control of AUVs with control input nonlinearities using reinforcement learning. IEEE Trans. Syst. Man Cybern. Syst. 47 (6), 1019–1029.
Ding, S., Park, J.H., Chen, C., 2020. Second-order sliding mode controller design with output constraint. Automatica 112, 108704.
Du, H., Wen, G., Cheng, Y., Lu, W., Huang, T., 2019. Designing discrete-time sliding mode controller with mismatched disturbances compensation. IEEE Trans. Ind. Inform. 16 (6), 4109–4118.
Edwards, C., Spurgeon, S., 1998. Sliding Mode Control: Theory and Applications. Crc Press.
Fierro, R., Lewis, F.L., 1998. Control of a nonholonomic mobile robot using neural networks. IEEE Trans. Neural Netw. 9 (4), 589–600.
Fossen, T.I., 2002. Marine Control Systems. Marine Cybernetics, Trondheim, Norway.
Fossen, T.I., Breivik, M., Skjetne, R., 2003. Line-of-sight path following of underactuated marine craft. In: Proceedings of the 6th IFAC Conference on Manoeuvring and Control of Marine Craft. pp. 211–216.
Ghommam, J., Ferik, S.E., Saad, M., 2018. Robust adaptive path-following control of underactuated marine vessel with off-track error constraint. Internat. J. Systems Sci. 49 (7), 1540–1558.
Hao, L., Zhang, H., Li, H., Li, T., 2020. Sliding mode fault-tolerant control for unmanned marine vehicles with signal quantization and time-delay. Ocean Eng. 215, 107882.
He, W., Yin, Z., Sun, C., 2016. Adaptive neural network control of a marine vessel with constraints using the asymmetric barrier Lyapunov function. IEEE Trans. Cybern. 47 (7), 1641–1651.
Hou, H., Yu, X., Fu, Z., 2020. Sliding-mode control of uncertain time-varying systems with state delays: A non-negative constraints approach. IEEE Trans. Syst. Man Cybern. Syst. http://dx.doi.org/10.1109/TSMC.2020.3029086.
Hu, X., Wei, X., Zhu, G., Wu, D., 2020. Adaptive synchronization for surface vessels with disturbances and saturated thruster dynamics. Ocean Eng. 216, 107920.
Laghrouche, S., Harmouche, M., Chitour, Y., Obeid, H., Fridman, L.M., 2021. Barrier function-based adaptive higher order sliding mode controllers. Automatica 123, 109355.
Lewis, F.L., Yesildirek, A., Liu, K., 1996. Multilayer neural-net robot controller with guaranteed tracking performance. IEEE Trans. Neural Netw. 7 (2), 388–399.
Liu, J., Wang, C., Cai, X., 2020. Adaptive neural network finite-time tracking control for a class of high-order nonlinear multi-agent systems with powers of positive odd rational numbers and prescribed performance. Neurocomputing 419, 157–167.
Mu, C., Ni, Z., Sun, C., He, H., 2016. Air-breathing hypersonic vehicle tracking control based on adaptive dynamic programming. IEEE Trans. Neural Netw. Learn. Syst. 28 (3), 584–598.
Ngo, K.B., Mahony, R., Jiang, Z., 2005. Integrator backstepping using barrier functions for systems with multiple state constraints. In: Proceedings of the 44th IEEE Conference on Decision and Control. pp. 8306–8312.
Obeid, H., Fridman, L., Laghrouche, S., Harmouche, M., 2018. Barrier function-based adaptive sliding mode control. Automatica 93, 540–544.
Obeid, H., Laghrouche, S., Fridman, L., 2021. Dual layer barrier functions based adaptive higher order sliding mode control. Int. J. Robust Nonlinear 31 (9), 3795–3808.
Obeid, H., Laghrouche, S., Fridman, L., Chitour, Y., Harmouche, M., 2020. Barrier function-based adaptive super-twisting controller. IEEE Trans. Automat. Control 65 (11), 4928–4933.
Plestan, F., Shtessel, Y., Brégeault, V., Poznyak, A., 2010. New methodologies for adaptive sliding mode control. Internat. J. Control 83 (9), 1907–1919.
Qiao, L., Zhang, W., 2019. Trajectory tracking control of AUVs via adaptive fast nonsingular integral terminal sliding mode control. IEEE Trans. Ind. Inf. 16 (2), 1248–1258.
Rout, R., Cui, R., Han, Z., 2020. Modified line-of-sight guidance law with adaptive neural network control of underactuated marine vehicles with state and input constraints. IEEE Trans. Control Syst. Technol. 28 (5), 1902–1914.
Shtessel, Y., Edwards, C., Fridman, L., Levant, A., 2014. Sliding Mode Control and Observation. Springer New York, New York, NY.
Skjetne, R., Smogeli, Ø., Fossen, T.I., 2004. Modeling, identification, and adaptive maneuvering of Cybership II: A complete design with experiments. IFAC Proc. Vol. 37 (10), 203–208.
Sun, B., Cao, Y., Guo, Z., Yan, Z., Wen, S., 2020. Synchronization of discrete-time recurrent neural networks with time-varying delays via quantized sliding mode control. Appl. Math. Comput. 375, 125093.
Sun, T., Pei, H., Pan, Y., Zhou, H., Zhang, C., 2011. Neural network-based sliding mode adaptive control for robot manipulators. Neurocomputing 74 (14–15), 2377–2384.
Tee, K.P., Ge, S., Tay, E.H., 2009. Barrier Lyapunov functions for the control of output-constrained nonlinear systems. Automatica 45 (4), 918–927.
Utkin, V., 2013. Sliding Modes in Control and Optimization. Springer Science & Business Media.
Wang, S., Cao, Y., Huang, T., Chen, Y., Li, P., Wen, S., 2020. Sliding mode control of neural networks via continuous or periodic sampling event-triggering algorithm. Neural Netw. 121, 140–147.
Wang, Y., Han, Q., 2018. Network-based modelling and dynamic output feedback control for unmanned marine vehicles in network environments. Automatica 91, 43–53.
Wang, D., Huang, J., 2005. Neural network-based adaptive dynamic surface control for a class of uncertain nonlinear systems in strict-feedback form. IEEE Trans. Neural Netw. 16 (1), 195–202.
Wang, N., Pan, X., 2019. Path following of autonomous underactuated ships: A translation–rotation cascade control approach. IEEE/ASME Trans. Mechatronics 24 (6), 2583–2593.

Wang, G., Wang, C., Li, L., Du, Q., 2016. Distributed adaptive consensus tracking control of higher-order nonlinear strict-feedback multi-agent systems using neural networks. Neurocomputing 214, 269–279.

Wu, D., Ren, F., Qiao, L., Zhang, W., 2018. Active disturbance rejection controller design for dynamically positioned vessels based on adaptive hybrid biogeography-based optimization and differential evolution. ISA Trans. 78, 56–65.

Xiang, X., Yu, C., Zhang, Q., 2017. Robust fuzzy 3D path following for autonomous underwater vehicle subject to uncertainties. Comput. Oper. Res. 84, 165–177.

Yan, Y., Yu, S., 2018. Sliding mode tracking control of autonomous underwater vehicles with the effect of quantization. Ocean Eng. 151, 322–328.

Yu, X., Feng, Y., Man, Z., 2020. Terminal sliding mode control–an overview. IEEE Open J. Ind. Electron. Soc. http://dx.doi.org/10.1109/OJIES.2020.3040412.

Yu, H., Guo, C., Yan, Z., 2019. Globally finite-time stable three-dimensional trajectory-tracking control of underactuated UUVs. Ocean Eng. 189, 106329.

Zhang, J., Xiang, X., Zhang, Q., Li, W., 2020. Neural network-based adaptive trajectory tracking control of underactuated AUVs with unknown asymmetrical actuator saturation and unknown dynamics. Ocean Eng. 218, 108193.

Zheng, Z., Sun, L., 2016. Path following control for marine surface vessel with uncertainties and input saturation. Neurocomputing 177, 158–167.

Zhou, M., Feng, Y., Xue, C., Han, F., 2020. Deep convolutional neural network based fractional-order terminal sliding-mode control for robotic manipulators. Neurocomputing 416, 143–151.